Correlation of transducin photoaffinity labeling with the specific formation of intermolecular disulfide linkages in its α-subunit

ARTICLE *in* BIOCHIMIE · NOVEMBER 2014

Impact Factor: 2.96 · DOI: 10.1016/j.biochi.2014.11.006 · Source: PubMed

3 AUTHORS, INCLUDING:

Carolina Moller

Florida International University

22 PUBLICATIONS **205** CITATIONS

SEE PROFILE

Jose Bubis

Simon Bolívar University

77 PUBLICATIONS **929** CITATIONS

SEE PROFILE

Biochimie 108 (2015) 120–132

Contents lists available at ScienceDirect

Biochimie

journal homepage: www.elsevier.com/locate/biochi

Research paper

Correlation of transducin photoaffinity labeling with the specific formation of intermolecular disulfide linkages in its α-subunit

Deisy Perdomo, Carolina Möller [1], José Bubis*

Departamento de Biología Celular, Universidad Simón Bolívar, Apartado 89.000, Valle de Sartenejas, Caracas 1081-A, Venezuela

ARTICLE INFO

Article history:
Received 18 August 2014
Accepted 8 November 2014
Available online 15 November 2014

Keywords:
Transducin
Photoaffinity labeling
Disulfide bonding
Oligomerization
Visual process

ABSTRACT

Transducin (T) is a heterotrimer of Tα, Tβ, and Tγ subunits. In the presence of light-activated rhodopsin, 8-azidoguanosine triphosphate (8-N_3GTP) was covalently incorporated into T in a UV-light photodependent manner, with a low stoichiometry of 0.02 mol of 8-N_3GTP per mol of T. Although Tα was preferentially labeled by 8-N_3GTP, Tβ and Tγ were also modified. Photolabeling of T was specifically inhibited by GDP and GTP, but not by β,γ-imido-guanosine 5′-triphosphate (GMP-PNP), indicating that 8-N_3GTP was modifying the GDP binding site of the holoenzyme. This was consistent with the observation that the photoaffinity probe was completely hydrolyzed to 8-N_3GDP by T activated by illuminated rhodopsin. The formation of intermolecular disulfide associations in T was also determined because photolabeling of T was performed under non-reducing conditions. We established that Cys-347 of Tα was the major residue involved in the formation of disulfide-linked T oligomers. Other cysteines of Tα, such as Cys-321, also participated in the formation of disulfide bonds, revealing a complex pattern of intermolecular disulfide cross-links that led to the polymerization of T. The spontaneous generation of these cystines in Tα inhibited the light-dependent GTPase and GMP-PNP binding activities of T. A model was constructed illustrating that when two heterotrimers dimerize through the formation of disulfide bridges between the Cys-347 of their Tα subunits, the guanine ring of the 8-N_3GDP bound to one T molecule might approach to the Tβγ-complex of the other heterotrimer. This model provides an explanation for the additional photolabeling of Tβ and Tγ by 8-N_3GTP.

1. Introduction

The photoreceptor protein rhodopsin (Rho) mediates scotopic vision. Rho is a G protein-coupled membrane receptor composed of the apoprotein opsin, and a covalently linked 11-*cis*-retinal chromophore [1]. Absorption of light produces the isomerization of the 11-*cis*-retinal chromophore to its all-*trans* configuration, causing conformational changes in Rho that lead to the formation of the active photointermediate metarhodopsin II (meta II). Meta II stimulates the retinal heterotrimeric G protein transducin (T) by catalyzing its GTP/GDP exchange activity, which initiates structural changes in the protein that produce the dissociation of the GTP-bound α-subunit (Tα) from the βγ-complex (Tβγ). Tα-GTP, in turn, activates a potent cGMP phosphodiesterase known as PDE6. The reduction in intracellular cGMP concentration leads to the closing of cGMP-gated cation channels in the plasma membrane of the rod cell, which causes a graded hyperpolarization of the photoreceptor cell and the generation of a neuronal signal.

Abbreviations: Rho, Rhodopsin; meta II, metarhodopsin II; T, transducin; Tα, transducin α-subunit; Tβ, transducin β-subunit; Tγ, transducin γ-subunit; 8-N_3GTP, 8-azidoguanosine triphosphate; IAA, iodoacetic acid; GMP-PNP, β,γ-imido guanosine 5′-triphosphate; TPCK, tosylphenyl alanyl chloromethyl ketone; PTH, phenylthiohydantoin; CHAPS, 3-[(3-cholamidopropyl) dimethylammonio]-1-propanesulfonate; PC, phosphatidylcholine; DTT, dithiothreitol; β-ME, β-mercaptoethanol; TFA, trifluoroacetic acid; DM, *n*-dodecyl-β-D-maltoside; ROS, rod outer segments; SDS, sodium dodecyl sulfate; SDS-PAGE, polyacrylamide gel electrophoresis in the presence of SDS; GTPγS, guanosine 5′-[γ-thio] triphosphate.

* Corresponding author. Laboratorio de Química de Proteínas, Departamento de Biología Celular, División de Ciencias Biológicas, Universidad Simón Bolívar, Apartado 89.000, Valle de Sartenejas, Baruta, Caracas 1081-A, Venezuela. Tel.: +58 212 9064219; fax: +58 212 9063064.

E-mail addresses: deisyperdomo@usb.ve (D. Perdomo), carolina@rostonics.com (C. Möller), jbubis@usb.ve (J. Bubis).

[1] Present address: Department of Chemistry and Biochemistry, Florida International University, 11200 SW 8th St., Miami, FL 33199, USA.

http://dx.doi.org/10.1016/j.biochi.2014.11.006
0300-9084/

T is characterized by several functional sites, which include its subunits interaction domains, the Mg^{2+} and guanine nucleotide binding regions, and contact sites for several proteins of the visual cascade, such as Rho, PDE6, phosducin [2,3], and the complex between the regulator of the G protein signaling 9 and the type 5 G protein β-subunit [4,5]. Group-specific labeling and chemical cross-linking techniques have been employed to identify and characterize functional residues in T [6–12]. A valuable approach to study ligand binding pockets in proteins has been to use specific analogs with systematically altered chemical properties in their structural moieties, in order to establish structure–activity relationships with regard to their functional groups. The nature of GTP binding to T has been investigated using several guanine nucleotide analogs. In early studies, 8-azidoguanosine triphosphate (8-N_3GTP) was employed to aid in the identification of the GTP binding subunit of T [13–15]. Hingorani et al. [16] have also used a battery of affinity and photoaffinity analogs with reactive groups attached to different positions of the GTP molecule to map the structure of the GTP-binding site of Tα. Other guanine nucleotide compounds such as phosphorothioate analogs have established the stereochemistry of the site [17]. GTP analogs with specific substitution on the γ-phosphate and the guanine ring have probed the stereoselectivity of nucleotide binding to T [18,19]. Pyridoxal 5′-phosphate and 5′-[p-(fluorosulfonyl)benzoyl] guanosine were also successfully employed as affinity reagents to covalently modify the active site of T [20,21]. In addition, exchange-inert Cr (III) β,γ-bidentate-guanine nucleotide complexes have been employed to probe the interaction of divalent metal ions with the guanine nucleotide [22]. To continue the studies on the structure-function of T, we have performed additional affinity tagging of T with 8-N_3GTP to correlate photolabeling with the spontaneous formation of intermolecular disulfide bridges in Tα.

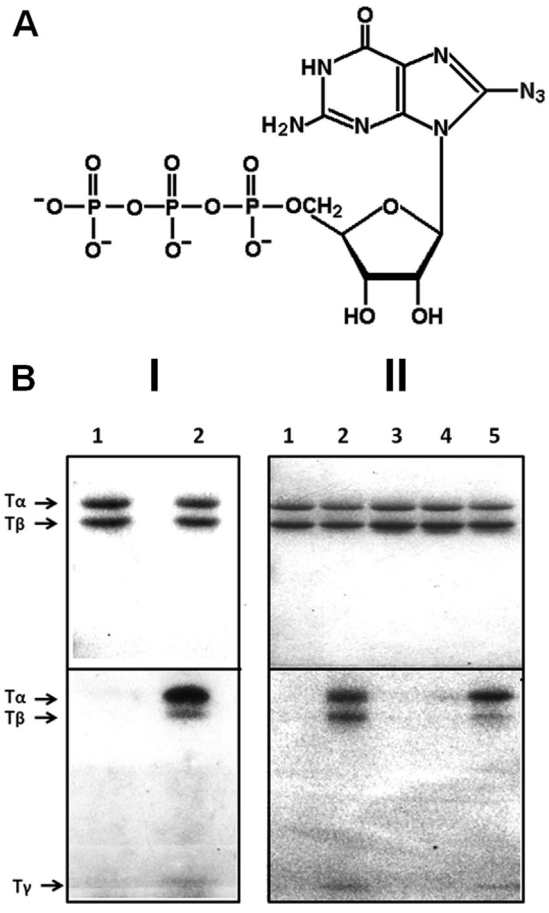

Fig. 1. A, Chemical structure of 8-azidoguanosine triphosphate. B, Analysis by SDS-PAGE of the covalent labeling of T with 8-N_3-[α-^{32}P] GTP. Panel I, Ultraviolet light-dependent incorporation of 8-N_3GTP into T. Samples of T were incubated with 8-N_3-[α-^{32}P] GTP in the presence of Rho. The reaction mixtures were irradiated (lane 2) or not (lane 1) with UV light, and separated by SDS-PAGE. Panel II, Incorporation of 8-N_3GTP into T in the presence of GDP, GTP or GMP-PNP. Samples of T were pre-incubated with GDP (lane 3), GTP (lane 4) or GMP-PNP (lane 5), in the presence of Rho. Control experiments of T in the absence of guanine nucleotides were also included (lanes 1 and 2). Then, all samples were incubated with 8-N_3-[α-^{32}P] GTP in the presence of photolyzed Rho, and irradiated (lanes 2–5) or not (lane 1) with ultraviolet light. (Top) Protein staining with Coomassie blue; (bottom) autoradiogram.

8-N_3GTP (Fig. 1A) is an arylazide photoreactive analog of GTP. The azide group is chemically inert, but it may be converted into a highly reactive nitrene by photolysis with UV light (λ = from 240 to 320 nm). This nitrene intermediate has the potential to form stable covalent bonds with almost any amino acid side chain in the protein. As previously reported [16], we also observed here that 8-N_3GTP was capable of modifying the three subunits of T although Tα was the major target. Inhibition experiments using guanine nucleotides suggested that 8-N_3GTP was modifying the GDP binding site of T. Some of our preliminary results that were presented in the Tenth International Conference on Methods in Protein Structure Analysis [7] have shown the generation of intermolecular disulfide linkages in Tα. Therefore, we explored the trapping of T oligomers by disulfide cross-linking in order to understand the labeling with 8-N_3GTP of the three subunits of T. We demonstrated the spontaneous formation of interchain disulfide bridges between Tα molecules, mainly involving their Cys-347 residues and other cysteines such as Cys-321. A model was then constructed on the basis of the dimerization and oligomerization of T that offered an explanation for the photolabeling with 8-N_3GTP of Tα, Tβ, and Tγ.

2. Material and methods

2.1. Materials

Bovine eyes were obtained from the nearest slaughterhouse (Beneficiadora Diagon, C.A., Matadero Caracas, Venezuela). Retinae were extracted in the dark, under red light, and were maintained frozen at −80 °C. Reagents were purchased from the following sources: 8-N_3 [α-^{32}P] GTP (17.3 Ci/mmol), and ω-amino octyl agarose, ICN Biomedicals; [2-^{3}H] iodoacetic acid ([^{3}H] IAA, 131 mCi/mmol), [γ-^{32}P] GTP (30 Ci/mmol), [α-^{32}P] GTP (30 Ci/mmol), and β,γ-imido-[^{3}H] guanosine 5′-triphosphate ([8-^{3}H] GMP-PNP) (15.6 Ci/mmol), Amersham; nitrocellulose filters type HA (0.45 μm), Millipore; diethylaminoethylcellulose DE 52, and glass fiber paper GF/C, Whatman; blue agarose, Bethesda Research Laboratories; tosylphenyl alanyl chloromethyl ketone (TPCK)-treated trypsin, phenylthiohydantoin (PTH)-carboxymethyl cysteine, 3-[(3-cholamidopropyl) dimethylammonio]-1-propane-sulfonate (CHAPS), egg phosphatidylcholine (PC, 99%), β-mercaptoethanol (β-ME), and dithiothreitol (DTT), Sigma: OptiPhase Hisafe II (scintillation liquid), LKB; trifluoroacetic acid (TFA, sequanal grade), Pierce; acetonitrile (HPLC grade), Fisher Scientific; iodoacetic acid (IAA), Kodak; *n*-dodecyl-β-D-maltoside (DM), Anatrace; Polygram Cel 300 PEI pre-coated plastic sheets for thin layer chromatography or PEI-cellulose (0.1 mm cellulose MN 300 polyethyleneimine impregnated), Macherey–Nagel + Co. 1D4-Sepharose and 1′-18′ competing synthetic peptide (corresponding to the carboxyl terminal 18 amino acids of Rho, sequence = $^+$H$_3$N-Asp-Glu-Ala-Ser-Thr-Thr-Val-Ser-Lys-Thr-Glu-Thr-Ser-Gln-Val-Ala-Pro-Ala-COO$^-$) were the generous gift of Dr. Barry Knox, State University of New York, Syracuse, USA. All other chemical compounds were of analytical grade.

2.2. Preparation of rod outer segments and washed membranes

Rod outer segments (ROS) were isolated from frozen bovine retinae by flotation and subsequent centrifugation on discontinuous sucrose gradients [23]. Urea-washed ROS membranes were prepared accordingly with Shichi and Somers [24]. ROS membranes and urea-washed ROS membranes were stored in the dark under argon at −80 °C. Rho concentration was calculated from its UV/visible absorption spectra, using the molar extinction coefficient of the protein [25].

2.3. Purification of detergent-solubilized Rho by batchwise immunoaffinity chromatography on 1D4-Sepharose

The 1D4-Sepharose resin contains the monoclonal antibody 1D4 covalently bound, which recognizes the last 8 amino acids at the carboxy-terminus of Rho. The purification procedure was carried out in the dark according to Oprian et al. [26], with slight modifications. Briefly, dark-purified ROS were solubilized with 1% DM in Buffer I [50 mM Tris–HCl (pH 6.8), 100 mM NaCl, and 0.1 mM $CaCl_2$], by agitation on a rotating wheel for 30 min, at 4 °C. The sample was centrifuged at 100,000*g*, for 30 min, at 4 °C, and the supernatant was transferred to a different tube. An aliquot of a 1D4-Sepharose suspended resin (1:1) was added to the supernatant, and incubated on the rotating wheel for 4 h, at 4 °C. Rho bound to the resin was washed 3 times with 0.2% DM in Buffer I, and then was eluted by incubating the affinity matrix with an excess of 1′-18′ competing synthetic peptide in Buffer I containing 0.2% DM. This peptide contains the last 18 residues of Rho and has been shown to block the interaction between the protein and the 1D4 monoclonal antibody [27]. The eluate was centrifuged at 100,000*g* and the purified solubilized Rho was extensively dialyzed against 0.2% DM in Buffer I in order to eliminate the excess of peptide. Then, Rho was stored at −80 °C in the dark.

2.4. Purification of T and its subunits

T was purified from ROS membranes prepared under room light, using anion-exchange chromatography on DE 52 [28]. Tα and Tβγ were isolated to homogeneity by chromatography *in tandem* through blue agarose followed by ω-amino octyl agarose [28]. T, Tα and Tβγ were stored at −20 °C in storage buffer [20 mM Tris–HCl (pH 7.4), 5 mM magnesium acetate, 100 mM NaCl, 10 mM β-ME, 50% glycerol].

2.5. Guanine nucleotide binding and GTPase activities of T

The guanine nucleotide binding activity of T was measured by Millipore filtration assay using [α-^{32}P] GTP, 8-N_3 [α-^{32}P] GTP, or the nonhydrolyzable analog of GTP, [^{3}H] GMP-PNP. In all cases, the binding reaction was carried out in Buffer II [10 mM Hepes (pH 7.4), 100 mM NaCl, 10 mM magnesium acetate, and 5 mM β-ME] containing 0.13 μM Rho (as urea-washed ROS membranes), 0.2 μM of native or reconstituted T, and various concentrations of the nucleotides (0–1 μM). After an overnight incubation at 4 °C, under light, a 100-μl aliquot of the reaction mixture was transferred to a filter reservoir (0.45 μm Millipore HA filter) containing 5 ml of ice-cold Buffer II. The filters were washed under vacuum with 25 ml of additional buffer, placed in scintillation vials, dried, and counted in 8 ml of OptiPhase Hisafe II [9].

The GTP hydrolysis activity of T was followed kinetically as described in detail in Bubis [28]. GTPase assays were performed in Buffer II, at room temperature, using 0.4 μM of native or reconstituted T, 0.025 μM of detergent-solubilized Rho, 10 μM [γ-^{32}P] GTP, 0.01% DM, 0.0075% PC and 0.005% CHAPS [23].

2.6. Photoaffinity labeling of T with 8-N_3 [α-^{32}P] GTP

Prior to treatment with 8-N_3 [α-^{32}P] GTP, T was dialyzed against 25 mM sodium phosphate (pH 6.8) at 4 °C to remove β-ME. Then, T (5.87 μM) was incubated with 0.11 μM of 8-N_3 [α-^{32}P] GTP in 100 mM sodium phosphate (pH 6.8) and 5 mM magnesium acetate, in the absence or presence of 1.67 μM Rho (as urea-washed ROS membranes). Following incubation for 2 h, at 4 °C, under 475 nm-filtered light, the samples were irradiated with an ultraviolet lamp (254 nm) for 10 min, at 4 °C. The covalent incorporation of 8-N_3 [α-^{32}P] GTP after photolysis was measured by TCA precipitation (10%) followed by filtration through GF/C glass fiber filters. Parallel experiments were performed with samples of T that were pre-incubated with either 1 mM GDP, 1 mM GTP or 1 mM GMP-PNP for 2 h, at 4 °C, under 475 nm-filtered light, in the absence or presence of Rho, prior to the addition of 8-N_3 [α-^{32}P] GTP. The photolabeling reactions were terminated with sample buffer [29], and the samples after separation by polyacrylamide gel electrophoresis in the presence of SDS (SDS-PAGE) were analyzed by autoradiography.

On a preparative scale, T (4.25 μM) was incubated with 7.3 μM Rho (as urea-washed ROS membranes) and 4 μM 8-N_3 [α-^{32}P] GTP, in the absence or presence of 1 mM GDP, and using the same conditions described above. After photolysis, the membranes containing the bleached Rho were removed by centrifugation at 40,000 rpm, for 30 min, using a Sorvall RCM120 micro-ultracentrifuge (RP120AT-203 fixed angle rotor). The supernantant containing the 8-N_3 [α-^{32}P] GTP-labeled T was incubated with trypsin at 37 °C overnight with 1:50 (w/w) TPCK-treated trypsin to protein. The reaction mixture was lyophilized, redissolved, and the resulting tryptic peptides were resolved by high-performance liquid chromatography (HPLC).

2.7. Spontaneous disulfide cross-linking of Tα

Tα was dialyzed either against 25 mM sodium phosphate (pH 6.8) or 85 mM Hepes (pH 8.0), containing 5 mM magnesium acetate. Control experiments were carried out in the same buffers but in the presence of 5 mM β-ME. Tα was then incubated with Tβγ to reform the holoenzyme, and the light-dependent [^{3}H] GMP-PNP binding and GTP-hydrolytic activities of the reconstituted protein were determined in the absence or presence of 2 mM DTT. Similar experiments were performed with heterotrimeric T.

To isolate the peptides containing the Cys residues involved in the spontaneous formation of disulfide linkages, a sample of Tα (0.15 mg) was dialyzed against 25 mM sodium phosphate (pH 6.8), and 5 mM magnesium acetate, at 4 °C, to eliminate β-ME. Then, Tα was modified with 10.1 mM [^{3}H] IAA, in 85 mM Hepes (pH 8.0), at 30 °C, for 30 min, in the dark, under argon, in the absence or presence of 2 mM DTT. Reactions were terminated by adding an excess of β-ME (118 mM) and the samples were dialyzed exhaustively against 50 mM NH_4HCO_3, and 2 mM EDTA (pH 7.7). Alkylated Tα was digested with TPCK-treated trypsin and the resulting peptides were subjected to HPLC separation.

2.8. Isolation of tryptic peptides by HPLC

HPLC was carried out on a Hewlett–Packard HP 1090 Liquid Chromatograph instrument using either a Rainin Microsorb C_{18} column (0.46 × 15 cm) or a Vydac C_{18} column (0.46 × 25 cm). The solvents employed were 10 mM sodium phosphate (pH 6.8) in vessel A and acetonitrile in vessel B. For the samples of T modified with 8-N_3 [α-^{32}P] GTP, the tryptic peptides were eluted isocratically in buffer A for 20 min, followed by a 120-min linear gradient from 0 to 60% B, using a Rainin Microsorb C_{18} column and a flow rate of 1 ml/min.

Tryptic peptides originated from carboxymethylated T were separated by using an initial 10-min isocratic wash and then a 180-min linear gradient from 0 to 40% B, followed by a 30-min linear gradient from 40 to 60% B. In this case, a Vydac C_{18} column was employed with a flow rate of 1 ml/min. Peptide bond absorbance was monitored at 210 nm and radioactive peptides were identified by scintillation counting. Prior to sequencing, the peptides were rechromatographed on a Vydac C_{18} column using a different solvent system: 0.1% trifluoroacetic acid (pH 2.13) in vessel A and 0.1% trifluoroacetic acid in acetonitrile in vessel B. The peptides were eluted with an 80-min linear gradient from 0 to 40% B, followed by a 20-min linear gradient from 40 to 100% B, employing a flow rate of 1 ml/min.

2.9. Peptide sequencing

Tryptic peptides of interest were subjected to gas-phase sequencing on an Applied Biosystems protein sequenator. PTH-amino acids were identified by HPLC, as described by Matsudaira [30].

2.10. Other procedures

Protein concentration was measured according to Bradford [31], using bovine serum albumin as protein standard. SDS-PAGE was carried out on 1.5-mm thick slab gels containing 12.5% polyacrylamide [29]. Coomassie blue R-250 was used for protein staining. The integrity of the 8-N_3 [α-^{32}P] GTP employed in the guanine nucleotide binding assay, before and after incubation with T and illuminated Rho, was analyzed by PEI-cellulose thin layer chromatography using 1 M potassium phosphate (pH 3.4) as the solvent.

3. Results

3.1. Photoaffinity labeling of T with 8-N_3 [α-^{32}P] GTP

In an attempt to map its guanine nucleotide binding site, T was incubated with 8-N_3 [α-^{32}P] GTP in the presence of photoactivated Rho. Fig. 1B (Panel I) shows that 8-N_3 [α-^{32}P] GTP was covalently incorporated into T following illumination with UV light. Although Tα was predominantly modified by the reagent, the other subunits of T, Tβ and Tγ, were also photolabeled to a less significant extent. Comparable experiments were performed in the presence of either 1 mM GDP, GTP or GMP-PNP (Fig. 1B, Panel II). Both GDP and GTP blocked the incorporation of 8-N_3 [α-^{32}P] GTP into the three subunits of T (Fig. 1B, Panel II). These results clearly indicated that the photoaffinity probe was specifically modifying the guanine nucleotide binding site of the protein. However, GMP-PNP, which is a non-hydrolyzable analog of GTP, did not inhibit the photolabeling of T with 8-N_3 [α-^{32}P] GTP. These results suggested that 8-N_3GTP selectively modified the GDP binding site of the holoenzyme. The stoichiometry of covalent incorporation was measured by TCA precipitation, followed by filtration through GF/C glass fiber filters, yielding 0.02 mol of 8-N_3 [α-^{32}P] GTP incorporated per mol of T.

In order to understand the low incorporation of the photoaffinity probe to T, the 8-N_3 [α-^{32}P] GTP binding activity of T was measured by a Millipore filtration assay. As can be seen in Fig. 2A, almost no 8-N_3GTP was bound to T at the concentrations used (0–1 μM). These results suggested that the photoaffinity label was being hydrolyzed by the GTPase activity of T during the overnight incubation at 4 °C. As control experiments, [α-^{32}P] GTP and [^{3}H] GMP-PNP were also employed as binding ligands. Similar to the findings obtained with 8-N_3 [α-^{32}P] GTP, almost no [α-^{32}P] GTP was bound to T at the concentrations used (Fig. 2A). Binding of 8-N_3 [α-^{32}P] GTP and [α-^{32}P] GTP to T never reached a plateau, and values of 0.2–0.4 mol of guanine nucleotide were bound per mol of T at the highest concentration of the ligand (1 μM). In contrast, 1 mol of GMP-PNP was bound per mol of T, and saturation was acquired at 20–30 nM GMP-PNP (Fig. 2A). As previously reported [20], GMP-PNP did bind with high affinity to T showing a Kd of ~5 nM (Fig. 2A).

With the purpose of determining whether 8-N_3 [α-^{32}P] GTP was susceptible to hydrolysis by T, T was incubated for 2 h with 8-N_3 [α-^{32}P] GTP, at 4 °C, in the presence of Rho, and under 475-nm filtered light. The sample was then irradiated on ice with an UV light lamp (254 nm) for 10 min. Aliquots (1 μl) of either the original 8-N_3 [α-^{32}P] GTP, or the sample mixture, were chromatographed on PEI cellulose sheets. As shown in Fig. 2B, all the photoaffinity label was hydrolyzed in the sample mixture demonstrating that the integrity of 8-N_3 [α-^{32}P] GTP was not maintained following incubation with T in the presence of illuminated Rho. This result demonstrated that 8-N_3 [α-^{32}P] GTP was hydrolyzed to 8-N_3 [α-^{32}P] GDP and other products by Rho-activated T. Since [α-^{32}P] GTP and 8-N_3 [α-^{32}P] GTP were hydrolyzed by T during incubation, we were not able to determine the Kd of T for either of these compounds using the Millipore filtration assay.

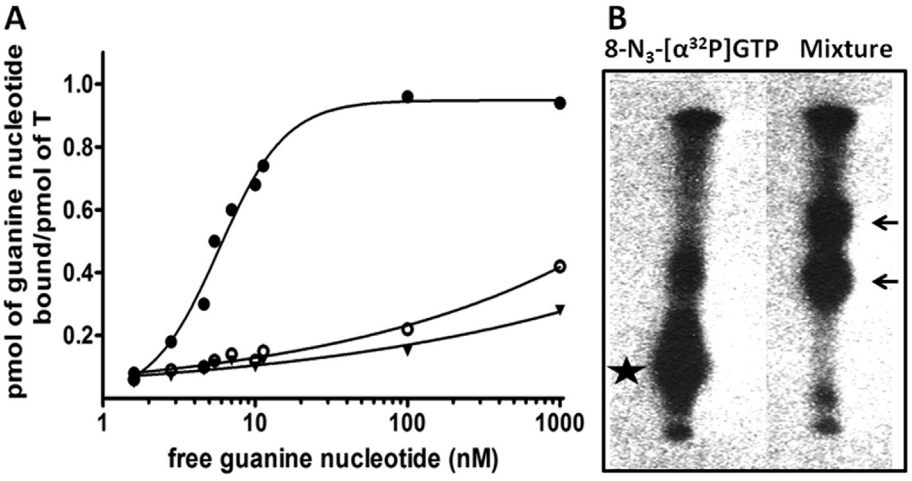

Fig. 2. A, Binding curves of T to [^{3}H] GMP-PNP, 8-N_3 [α-^{32}P] GTP or [α-^{32}P] GTP. Samples of T were incubated with various concentrations of [^{3}H] GMP-PNP (●), 8-N_3 [α-^{32}P] GTP (▼) or [α-^{32}P] GTP (○), in the presence of Rho. Guanine nucleotide binding was determined by Millipore filtration. B, PEI cellulose chromatography of 8-N_3 [α-^{32}P] GTP before and after incubation with T in the presence of Rho (Mixture). The star highlights the migration of an aliquot (1 μl) of the original 8-N_3 [α-^{32}P] GTP. Arrows indicate the migration of the hydrolyzing products of 8-N_3 [α-^{32}P] GTP following incubation with T and Rho (1 μl of the mixture).

T was covalently labeled with 8-N_3 [α-^{32}P] GTP on a preparative scale in the absence or presence of 1 mM GDP. After irradiation with UV light (254 nm), the specificity of the modification was assessed by digesting the covalently modified protein with TPCK-treated trypsin and resolving the resulting peptides by HPLC. As shown in Fig. 3, a broad radioactive peak was observed at the beginning of the chromatograms, which corresponded to the excess of free label as demonstrated by HPLC separations of aliquots of 8-N_3 [α-^{32}P] GTP through the same C_{18} reversed-phase column (data not shown). An additional radioactive peak corresponding to a tryptic peptide of T was also labeled with 8-N_3 [α-^{32}P] GTP (Fig. 3A). This peptide was specifically modified since it was not observed when the reaction was carried out in the presence of GDP (Fig. 3B). This result demonstrates that the photoaffinity probe is specifically tagging the guanine nucleotide binding site of T. Moreover, this radioactive peptide was not observed neither when the reaction was performed without UV light nor when illuminated Rho was absent from the reaction mixture (data not shown). Due to the small amount of radioactivity that was incorporated into the protein, we were not able of purifying the modified tryptic peptide and no information about its amino acid composition or sequence was obtained.

3.2. Spontaneous formation of disulfide bonds in Tα

As can be seen in Fig. 4A, higher molecular weight oligomers with apparent molecular masses of 70, 100, 130, 200 and >200 kDa were detected when samples of T and Tα were dialyzed at pH 6.8 to eliminate the β-ME, and electrophoresed under non-reducing conditions. Moreover, some cross-linked products did not penetrate the stacking gel (data not shown). In contrast, no high molecular weight polypeptide bands were obtained when Tβγ was electrophoresed in the absence of β-ME (Fig. 4A). Two-dimensional electrophoresis (non-reducing, reducing) showed that the bands of apparent molecular masses of 70, 100, 130, 200 and >200 kDa corresponded to Tα oligomers (Fig. 4B).

The effect on T function of the spontaneous oxidations of sulfhydryl groups in Tα was examined at different pH values and under non-reducing conditions. Dialysis of Tα at pH 8.0, followed by reconstitution with native Tβγ, produced the total inactivation of its GTPase activity (Fig. 5A). However, native GTP-hydrolytic activity was obtained after incubation of the reconstituted holoenzyme with 2 mM DTT. Dialysis of Tα at pH 6.8, followed by reconstitution with native Tβγ, produced only a reduction of about 30–40% in the T GTPase activity (Fig. 5A), and as before, the addition of 2 mM DTT restored the native T GTPase functionality. Tα dialyzed in the presence of 5 mM β-ME and reconstituted with intact Tβγ-complex, exhibited native GTP-hydrolytic capacity, in the presence or absence of 2 mM DTT (data not shown).

Dialysis at pH 8.0 under non-reducing conditions of the complete holoenzyme, or of Tα reconstituted with native Tβγ, also caused the total inactivation of the GMP-PNP binding capability of the protein (data not shown). This activity was completely restored in the presence of 5 mM β-ME (data not shown). A reduction of about 70% in GMP-PNP binding activity was observed following

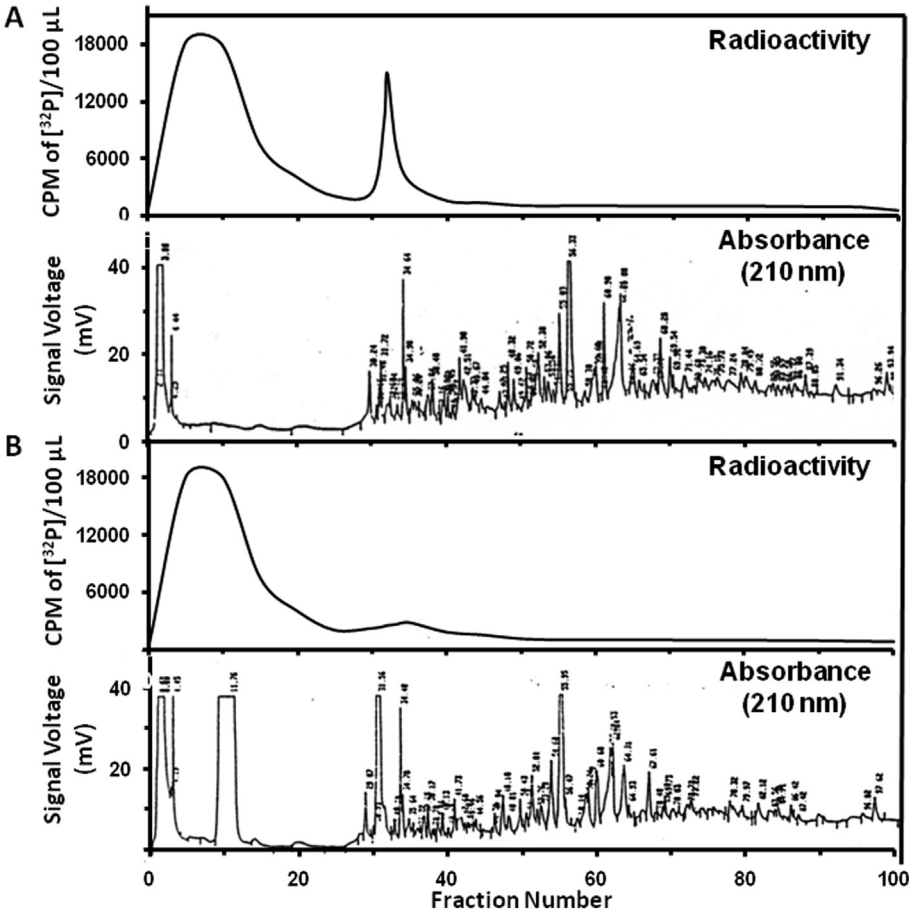

Fig. 3. HPLC separation of tryptic digest of 8-N_3 [α-^{32}P] GTP-modified T. T was incubated with 8-N_3 [α-^{32}P] GTP and photoactivated Rho in the absence (A) or presence (B) of GDP. Following irradiation with UV light, both samples were digested with TPCK-treated trypsin and the resulting peptides were separated by HPLC on a C_{18} column. (Top) Radioactivity (cpm of [^{32}P]); (bottom) absorbance at 210 nm.

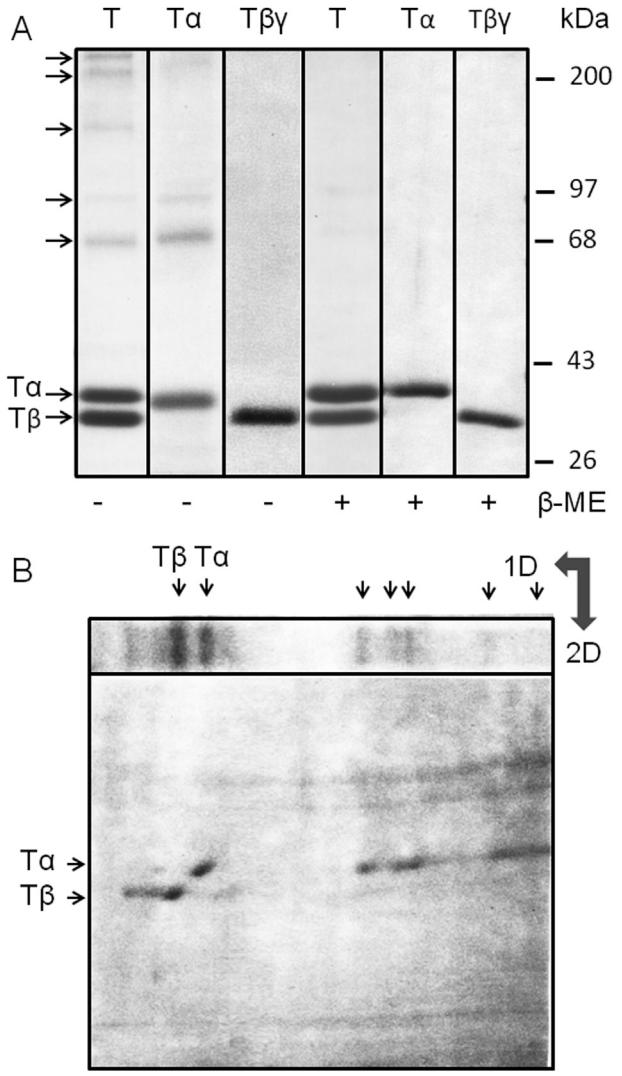

Fig. 4. Spontaneous formation of disulfide bonds in Tα. A, Samples of T, Tα and Tβγ were dialyzed to remove β-ME. Aliquots of T, Tα and Tβγ were electrophoresed in the absence (−) or in the presence (+) of β-ME. B, Two-dimensional electrophoresis of disulfide cross-linked T in the absence or presence of β-ME. The cross-linked sample was electrophoresed under non-reducing conditions in the first dimension (1D) and under reducing conditions in the second dimension (2D). Arrows indicate the migration of Tα, Tβ and the higher molecular weight oligomers of Tα.

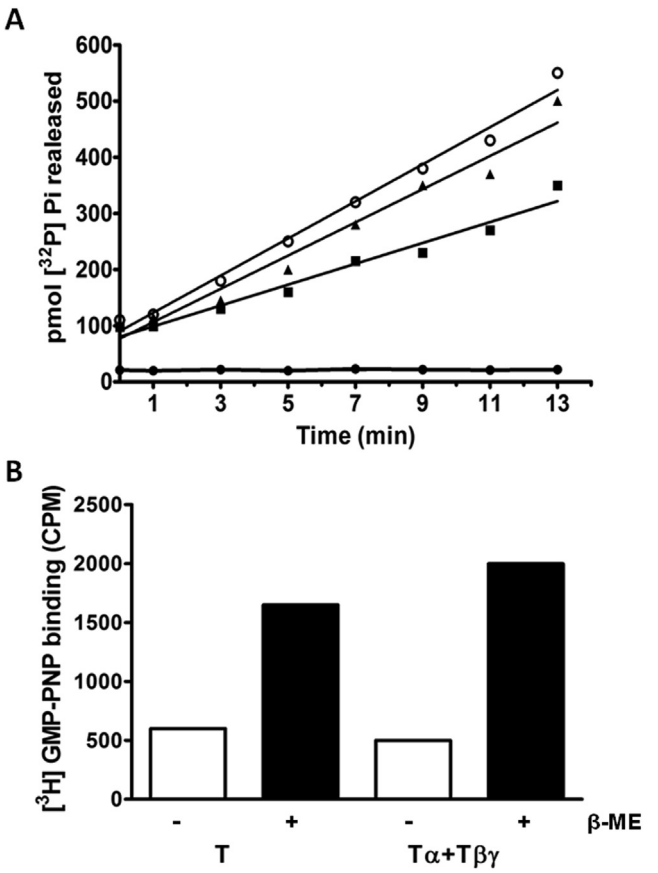

Fig. 5. A, GTPase activity of Tα dialyzed at pH 8.0 or pH 6.8 and reconstituted with Tβγ. Tα was dialyzed at pH 8.0 (●, ▲) or pH 6.8 (■, ○). Tα was then incubated with Tβγ to reform the holoenzyme, and the light-dependent GTP-hydrolytic activity of the reconstituted protein was determined in the absence (●, ■) or presence (▲, ○) of DTT. B, GMP-PNP binding activity of T dialyzed at pH 6.8 or Tα dialyzed at pH 6.8 and reconstituted with Tβγ, in the absence (−) or presence (+) of β-ME.

dialysis at pH 6.8 and under non-reducing conditions of T, or of Tα that has been regenerated with native Tβγ (Fig. 5B). The GMP-PNP binding activity was completely restored in the presence of 5 mM β-ME (Fig. 5B). All these results demonstrated the formation of disulfide bridges in Tα, which appeared to be responsible of the loss in T GTPase and GMP-PNP binding activities at neutral and basic pHs.

In order to localize the cysteines involved in the spontaneous formation of disulfide linkages, Tα was initially dialyzed at pH 6.8 to remove β-ME, and then was modified with [^{3}H] IAA at pH 8.0 in the absence or presence of 2 mM DTT. The stoichiometry of modification was found to be 1.4 and 2.7 pmol of IAA incorporated per pmol of Tα, in the unreduced and reduced samples, respectively. Alkylated samples were digested with TPCK-treated trypsin, and the generated products were separated by HPLC. Fig. 6 shows the radioactivity profiles obtained following HPLC separation of tryptic digests of [^{3}H] IAA-modified unreduced (Panel A) and reduced (Panel B) samples of disulfide-linked Tα. The major radioactive peptides were rechromatographed on a C_{18} reversed-phase HPLC column using a different buffer system (data not shown), and the purified carboxymethylated peptides were subjected to gas-phase sequencing. One peptide was modified by IAA independently of the presence of DTT in the reaction mixture (peptide II, Panel A and B) and corresponded to residues 129-138. Since the radioactivity was released at sequencing cycle 7, gas-phase sequencing of peptide II from both samples identified Cys-135 of Tα as the amino acid residue modified by IAA in the presence or absence of DTT (Table 1). The PTH-derivative, carrying the radioactivity, corresponded to PTH-carboxymethyl cysteine based on its coelution with a standard PTH-caboxymethyl cysteine. The accessibility of Cys-135 of Tα under both conditions demonstrated that this residue is not involved in the spontaneous formation of disulfide bonds in Tα. However, the sample containing the reducing agent showed three new major radioactively labeled peptides (peptides I, III, and IV), which must be involved in the disulfide-linked oligomerization of Tα (Fig. 6). Gas phase sequencing of peptides I (residues 346–350) and III (residues 342–350) showed that both contained Cys-347 of Tα, being peptide III an incomplete proteolytic cleavage of peptide I (Table 1). Both, PTH-carboxymethyl cysteine and radioactivity were released at sequencing cycle 2 in peptide I and sequencing cycle 6 in peptide III (Table 1). Trypsin is known to catalyze the hydrolysis of arginyl and lysyl peptide bonds at their carboxyl side; however, the presence of acidic residues on either side of the basic residue significantly reduces the rate of cleavage. Thus, incomplete trypsin

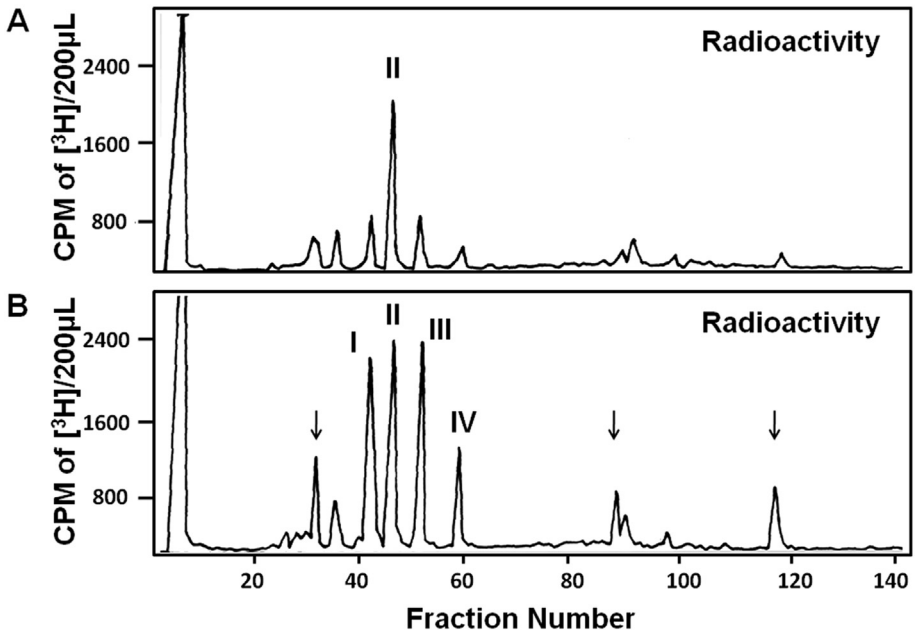

Fig. 6. HLPC separation of tryptic peptides from [^{3}H] IAA-modified Tα. Purified Tα was dialyzed exhaustively at pH 6.8 to remove β-ME and induce the formation of disulfide cross-links. Disulfide-linked Tα was incubated with [^{3}H] IAA in the absence (A) or presence (B) of DTT. Both samples were digested with TPCK-treated trypsin, and the generated products were separated by HPLC using a C_{18} column. Shown are the radioactivity profiles (cpm of [^{3}H]). The major radioactive peptides are designated with roman numbers. Arrows indicate additional radioactive peptides that might be involved in the formation of disulfide bonds in Tα.

digestions are expected to occur in peptides, like peptide III, which contain trypsin target sites followed by acidic amino acids. These results identified Cys-347 of Tα as one of the cysteines involved in the spontaneous formation of disulfide cross-links in Tα. Since PTH-carboxymethyl cysteine and radioactivity were released at step 8, sequence analysis of peptide IV (residues 314–322) identified Cys-321 of Tα as the carboxymethylated residue (Table 1). Hence, this cysteine also appeared to participate in the formation of disulfide bridges in Tα; however, the amount of [^{3}H] IAA incorporated onto peptide IV was about 30% of the total [^{3}H] IAA bound to Cys-347 in peptides I and III (Fig. 6). As also seen in Fig. 6, there are other minor [^{3}H]-containing tryptic peptides which might be involved in the formation of disulfide cross-links in Tα. One of these peptides might correspond to the one containing the Cys-210 residue of Tα, which was identified by utilizing either [^{125}I]-N-(3-iodo-4-azidophenylpropionamido-S-(2-thiopyridyl) cysteine [32] or lucifer yellow [33]. The radioactive peak eluting at the beginning of the chromatograms (fractions 4 to 6, Fig. 6) corresponded to unbound [^{3}H] IAA, as demonstrated by HPLC separations of aliquots of [^{3}H] IAA through the same C_{18} reversed-phase column (data not shown). Additionally, this peak was purified by rechromatography on a C_{18} reversed-phase HPLC and subjected to gas-phase sequencing. The isolated fractions did not yield any sequence signal after 10 Edman degradation cycles (data not shown).

4. Discussion

By using competitive displacement of [^{35}S] guanosine 5′-[γ-thio] triphosphate (GTPγS) binding to T with a series of guanine nucleotide analogs, Kelleher et al. [19] reported a Kd for GDP of 10 μM, an affinity that was approximately 30–100-fold lower than GTP and GTPγS. As shown here by thin layer chromatography on PEI cellulose sheets, 8-N_3 [α-^{32}P] GTP was completely hydrolyzed to 8-N_3 [α-^{32}P] GDP and other products by Rho-activated T. Then, the lower affinity of T for GDP can be extrapolated to 8-N_3GDP, and might justify the low stoichiometry of binding and the concomitant low covalent incorporation of the photoaffinity tag into T.

Since Tα, Tβ and Tγ were labeled by 8-N_3GTP, the tertiary structure of the heterotrimeric G protein was analyzed in order to evaluate whether the three subunits contained sites located in close proximity to the guanine ring of the nucleotide. Initially, we assumed that the folding of photolabeled T was analogous to that of T bound to GDP. An examination of the X-ray crystal structure of T bound to GDP [34] (Fig. 7A) showed that although the guanine nucleotide appears to be deeply buried in its binding pocket, Tα contains several residues that are near to the guanine ring of the GDP molecule and may account for the photolabeling of Tα by 8-N_3 [α-^{32}P] GTP. For example, Thr-44, Asn-265 and Ala-322 of Tα are located 3.47 Å, 3.92 Å and 4.35 Å, respectively, from the C-8 position of the guanine ring of the GDP bound to the heterotrimer (Fig. 7B). Yet, the side chains of these residues are not chemically very reactive, probably yielding the low covalent incorporation seen. In contrast, the Tβγ-complex is distant and inaccessible to the nucleotide binding site (Fig. 7A). The closest residues of Tβ (Fig. 7C) and Tγ (Fig. 7D) to the C-8 position of the GDP guanine ring are located at distances of about 22 Å and 30 Å, respectively (Trp-99, Leu-117, Asn-119 and Thr-143 of Tβ; and Leu-9, Thr-10 and Glu-11 of Tγ), thus making it highly unlikely that the three subunits would be modified by the same 8-N_3 [α-^{32}P] GTP molecule bound to the Tα subunit of one T heterotrimer. Lambright et al. [35] have shown that the structures of Tα-GDP and Tα-GTPγS are quite similar. The main structural differences induced by nucleotide exchange are localized to three adjacent regions on one face of Tα, which are referred as switch I, II and III, which only correspond to approximately 14% of the entire Tα structure. Neither Thr-44, nor Asn-265, nor Ala-322 of Tα are located within these switch regions, and these residues remained close to the C-8 position of the GTPγS guanine ring in the structure of Tα-GTPγS as well [36]. The observation that GMP-PNP was not capable of blocking the photoaffinity labeling of T with 8-N_3 [α-^{32}P] GTP strongly suggests that the conformational fold of Tα in the sample of T subjected to photolabeling differed from the

Table 1
Sequence analysis of tryptic peptides of disulfide-linked Tα modified by iodoacetic acid.[a]

Unreduced disulfide-linked Tα										
	129	130					135			138
Peptide II	Asp	Ser	Gly	Ile	Gln	Ala	Cys	Phe	Asp	Arg
Gas-phase sequencing	→	→	→	→	→	→	CMCys	→	→	→
Radioactivity (cpm/step)	23	18	26	28	21	19	513	112	30	23
Reduced disulfide-linked Tα										
	346				350					
Peptide I	Asp	Cys	Gly	Leu	Phe					
Gas-phase sequencing	→	CMCys	→	→	→					
Radioactivity (cpm/step)	15	481	123	35	20					
	129	130					135			138
Peptide II	Asp	Ser	Gly	Ile	Gln	Ala	Cys	Phe	Asp	Arg
Gas-phase sequencing	→	→	→	→	→	→	CMCys	→	→	→
Radioactivity (cpm/step)	37	43	45	35	44	43	622	133	43	39
	342			345					350	
Peptide III	Glu	Asn	Leu	Lys	Asp	Cys	Gly	Leu	Phe	
Gas-phase sequencing	→	→	→	→	→	CMCys	→	→	→	
Radioactivity (cpm/step)	31	28	27	25	31	523	98	30	35	
	314	315					320		322	
Peptide IV	Glu	Ile	Tyr	Ser	His	Met	Thr	Cys	Ala	
Gas-phase sequencing	→	→	→	→	→	→	→	CMCys	→	
Radioactivity (cpm/step)	23	26	30	21	18	20	21	188	65	

[a] Tα was dialyzed against 25 mM sodium phosphate (pH 6.8), 5 mM magnesium acetate, at 4 °C, to induce the formation of disulfide bonds. Disulfide-linked Tα was modified with [^{3}H] IAA in 85 mM Hepes (pH 8.0), at 30 °C, for 30 min, in the absence (unreduced) or presence (reduced) of 2 mM DTT. Alkylated Tα was digested with TPCK-treated trypsin and the resulting peptides were separated by HPLC (Fig. 6). Shown are the sequences of the major radioactive peptides that were found. Residues are numbered according to the published sequence of Tα. CMCys = carboxymethyl Cys.

reported structures of Tα-GDP and Tα-GTPγS. If that is the case, other residues of Tα, different than Thr-44, Asn-265 and Ala-322 may perhaps approach the C-8 position of the GDP guanine ring. The Tβγ-complex might also fold differently in the photolabeled T sample.

Tα consists of two easily delineated domains, a TαRas or GTPase domain and a TαAH helical domain, flanking a deep guanine nucleotide binding cleft [34–36] (Fig. 8A). Rasmussen et al. [37] reported the crystal structure of the active state ternary complex composed of agonist-occupied monomeric β_2 adrenergic receptor (β_2AR) and nucleotide-free Gs heterotrimer, the stimulatory G protein that activates adenylyl cyclase. Like Tα, the α-subunit of Gs ($G\alpha_s$) consists of $G\alpha_s$Ras and $G\alpha_s$AH domains. The most surprising observation in the β_2AR-Gs complex was the large displacement of $G\alpha_s$AH relative to $G\alpha_s$Ras, which consisted of a rotation of approximately 127° about the junction between the domains. When comparing the structure of $G\alpha_s$Ras from β_2AR-Gs with that from $G\alpha_s$-GTPγS [38], the largest difference was observed for the α5-helix, which is displaced 6 Å towards the receptor and rotated as the carboxyl terminal end projects into the transmembrane core of

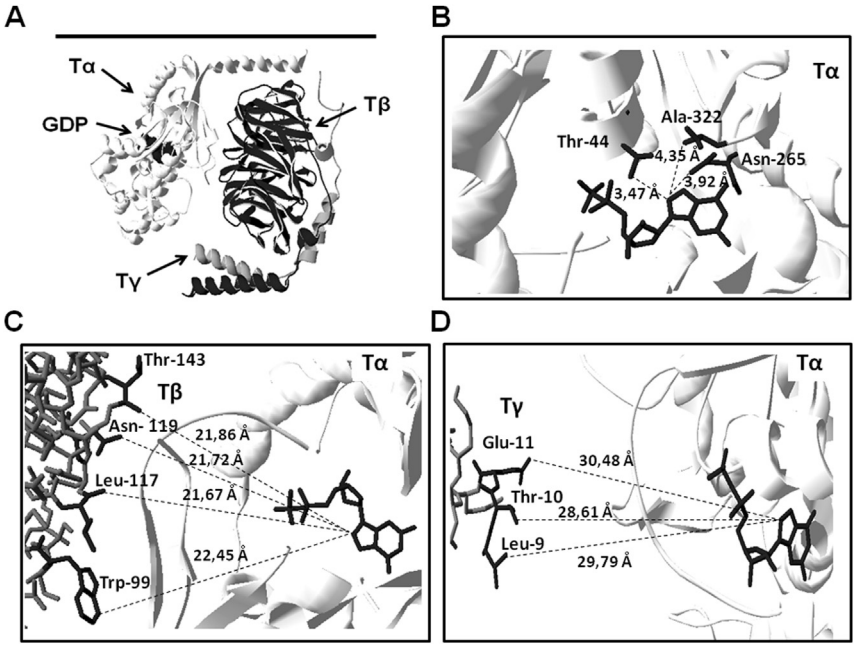

Fig. 7. A, Three dimensional schematic representation of the GDP-bound structure of heterotrimeric T using backbone and ribbon diagrams. Shown are the structures of Tα (light gray), Tβ (dark gray), and Tγ (gray) solved by X-ray diffraction (PDB ID: 1GOT) [34]. Alpha helices, β strands and non-repetitive coils or loops are represented by spring-shaped ribbons, arrows and lines or thin tubes, respectively. Bound GDP is highlighted in black. The hypothetical location of the membrane, which represents the active Rho-interacting surface of the heterotrimer, can be seen at the top (black line). The closest residues of Tα (B), Tβ (C) and Tγ (D) to the C-8 position of the guanine ring of the bound GDP are indicated, together with their corresponding distances.

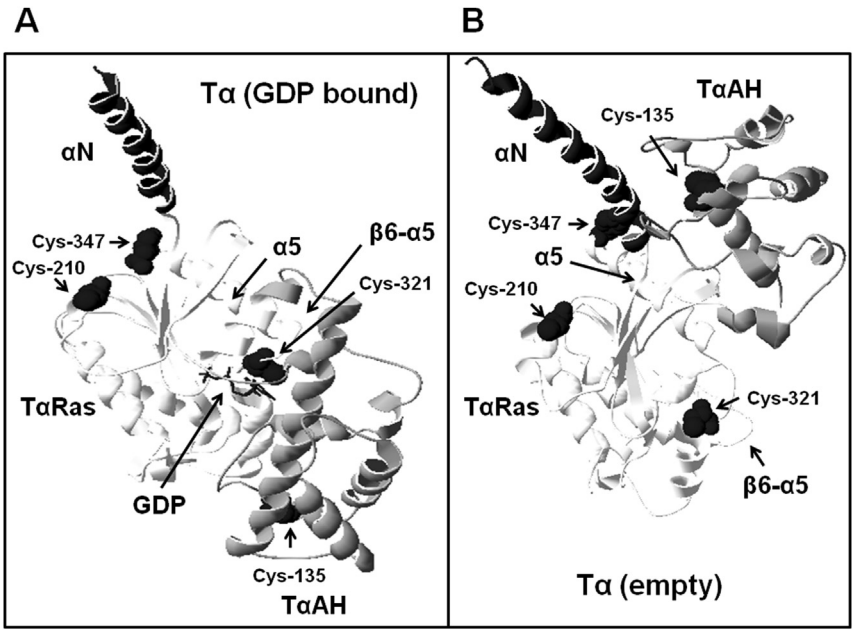

Fig. 8. Conformational changes in Tα. A comparison of GDP-bound Tα (A) with nucleotide-free Tα (B) is shown. The structure of GDP-bound Tα was obtained from the GDP-bound crystal structure of T (PDB ID: 1GOT) [34]. Free-nucleotide Tα was modeled using the structure of the empty $G\alpha_s$ in the β_2AR-Gs complex (PDB ID: 3SN6) [37]. Indicated are the GTPase domain (TαRas, light gray), the helical domain (TαAH, gray) and the N-terminal helix (αN, dark gray) of Tα. The TαAH domain in the nucleotide-free Tα exhibited a dramatic displacement relative to its position in the Tα GDP-bound state. Changes in the α5-helix (α5) of Tα were also seen in the empty state, perturbing the β6-α5 loop (β6-α5) which is part of the guanine nucleotide binding pocket in the GDP-bound state. The location of Cys-135, Cys-210, Cys-321 and Cys-347 are also identified in both conformations.

the β_2AR [37]. The α5-helix of $G\alpha_s$ docks into a cavity formed on the intracellular side of the receptor by the opening of transmembrane helices 5 and 6. Particularly, Tyr-391 of $G\alpha_s$, which coincidentally corresponds to Cys-347 in Tα, packs against Arg-131 of the conserved E/DRY sequence in transmembrane helix 3. Arg-131 also packs against Tyr of the conserved NPxxY sequence in transmembrane helix 7. Thus, the X-ray structure of β_2AR-Gs clearly illustrates that conformational links between the β_2AR and the nucleotide-binding pocket primarily involve the carboxyl terminal α5-helix of $G\alpha_s$. Interestingly; previous studies using a variety of approaches have demonstrated the important role of the α5-helix in G protein-coupled receptor-G protein interactions [39–42]. On the basis of the high degree of homology seen among G protein α-subunits, we modeled the nucleotide-free Tα conformation using the structure of the empty $G\alpha_s$ in the β_2AR-Gs complex as a framework (Fig. 8B). For comparison purposes, the location of the cysteine residues that are referred in the text in both GDP-bound Tα (Fig. 8A) and nucleotide-free Tα (Fig. 8B) are indicated.

As revealed here, intermolecular cystines between Tα subunits were spontaneously formed when T was dialyzed in the absence of reducing agents. Our results revealed distinct oligomeric forms of Tα protomers but not of the Tβγ-complexes of T. Wessling-Resnick and Johnson [43] also found that intermolecular disulfide bridges between the α-subunits of T molecules were spontaneously formed when the purified T was placed in a non-reducing buffer system. Given that photolabeling of T with 8-N_3GTP was performed under non-reducing conditions, dimers and oligomeric complexes of Tα must be clearly trapped through the formation of disulfide bonds in which Cys-347 of Tα appeared to be mainly involved. The oligomerization of T via disulfide linkages inhibited T function. Cys-347 has previously been recognized as the pertussis toxin-catalyzed ADP-ribosylation site in T [44], a modification that inactivated its light-dependent GTPase activity [45] by hindering the interaction of T with Rho. Cys-347 and Cys-210 of Tα have been reported as the two major labeling sites for [^{125}I] *N*-(3-iodo-4-azidophenyl propionamido)-*S*-(2-thiopyridyl) cysteine [32] and lucifer yellow [33]. The derivatization of both of these cysteines inhibited Rho-catalyzed activation of T. Moreover, when T was alkylated with IAA, Cys-347 of Tα was also recognized as the residue responsible for the complete inactivation of the protein [8]. Since Cys-347 is located in the α5-helix of Tα, all these evidences also demonstrate that the α5-helix of this subunit is a key element in enabling nucleotide exchange catalysis by Rho. Accordingly, the spontaneous formation of disulfide bonds involving the Cys-347 residues of Tα subunits in T oligomers would be predicted to induce a movement of the α5-helix of Tα, which would concomitantly change the conformation at the COOH terminus of this subunit. This movement probably would affect the affinity of T for guanine nucleotides causing the release of GDP, similar to what occurs in the structure of the β_2AR-Gs complex (Fig. 8B). These apparent conformational changes might explain the negative effects of disulfide formation on the GTPase and GMP-PNP binding activities of T. Consistently, the modification of T with IAA, which resulted in the specific carboxymethylation of Cys-347 of Tα, stabilized the free nucleotide conformation of T associated to light-activated Rho [8]. Yang et al. [33] also noted that conformational changes, taking place at the C-termini of Tα, during T activation, appeared to be important for allosteric communication between Rho-binding and GDP-binding sites on the molecule.

How are the Tβ and Tγ subunits modified by 8-N_3 [α-^{32}P] GTP? A model was constructed by dimerizing T heterotrimers through the formation of a disulfide bond involving the Cys-347 of each Tα subunit in the dimer (Fig. 9). If two T heterotrimers are aligned as shown in Fig. 9A and B, it is clearly possible for the guanine ring of the GDP bound to Tα of one T molecule to come into close proximity to the Tβγ-complex of the other heterotrimer. Connected with movement of the α5-helix, the β6-α5 loop, which interacts with the guanine ring in the $G\alpha_s$-GTPγS structure [38], is displaced outward in the β_2AR-Gs structure (Fig. 8B), away from the nucleotide-binding pocket [37]. Since other cysteines of Tα, such as Cys-321, were proven to also participate in the spontaneous formation of disulfide cross-links, a complex pattern of intermolecular cystines

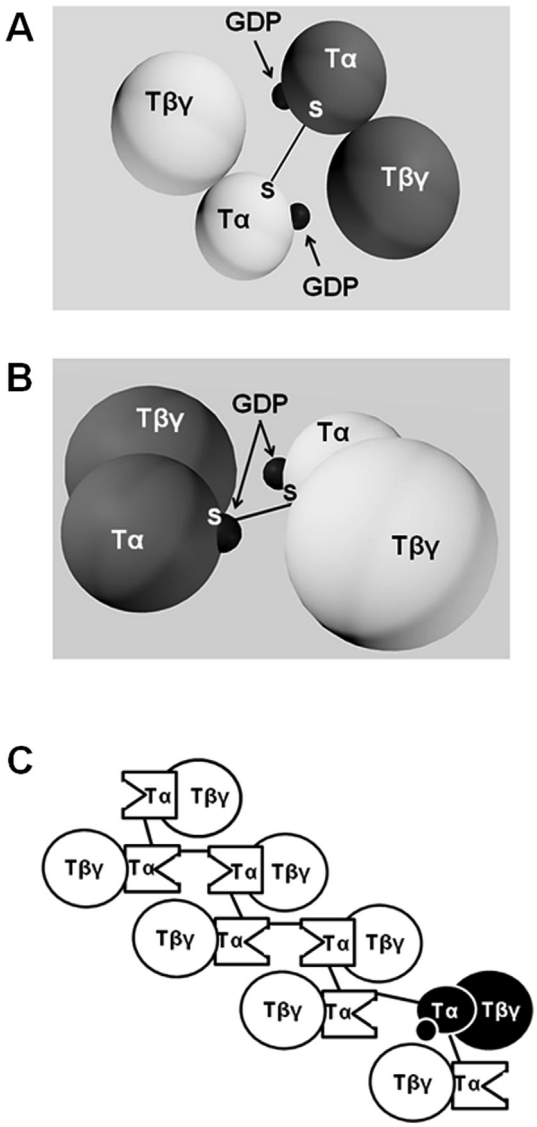

Fig. 9. Top (A) and frontal views (B) of a proposed dimer of T heterotrimers generated by a disulfide bridge between the Cys-347 residues of each of their Tα subunits. Tα and Tβγ, are modeled as spheres. One heterotrimer is colored in light gray and the second heterotrimer is colored in dark gray. Bound GDP is shown in black. S–S = disulfide bond. C, Disulfide-linked T oligomers. Shown is an example of an oligomer constituted by four dimers of T heterotrimers. Most T heterotrimers in the oligomer are shown with their Tα subunits in the conformation carrying the empty nucleotide-binding site (white). However, some T molecules might possess their Tα protomers in the bound guanine nucleotide conformation. This is illustrated by one T (black); the small black circle represents the 8-N_3GDP bound to this heterotrimer. Intermolecular disulfide linkages (–).

can be proposed to explain the oligomerization of T. Interestingly, Cys-365 of $G\alpha_s$, which corresponds to Cys-321 in Tα, is located in the β6-α5 loop [37] and becomes more accessible in the nucleotide-free conformation of the protein (Fig. 8B). In contrast, cross-linking of Cys-321 of Tα does not appear to be easily available for disulfide formation in the GDP bound form of T [34] (Fig. 8A). Additionally, if we are in the presence of a new structural fold of T, the guanine ring of the GDP bound to Tα might be sitting on the surface of the protein and might draw closer to the Tβγ-complex of a second T heterotrimer. Fig. 9C illustrates a disulfide-linked T oligomer composed of four dimers of T heterotrimers as an example. As proposed above, most Tα subunits in the oligomer are shown with an empty nucleotide-binding pocket (Fig. 9C, in white). However, since ~30% of GMP-PNP binding activity and ~65% of GTPase activity remained in the Tα sample that was dialyzed at pH 6.8, and reconstituted with intact Tβγ-complex, some of the 8-N_3 [α-^{32}P] GDP that results from the hydrolysis of the original photoaffinity probe is capable of binding to a number of Tα protomers, as illustrated with one T heterotrimer in the figure (Fig. 9C, in black). Then, some Tα subunits will contain bound guanine nucleotides. The movement of the α5-helix is also associated with other changes involving interactions between this helix and the β6-strand, the αN-β1 loop, and the α1-helix [37]. The labeling of T with 8-N_3GTP therefore not only provides information about nucleotide binding to Tα but also potentially provides information as to how the heterotrimers might be oriented with respect to one another in the T oligomers that are spontaneously formed in the absence of reducing agents (Fig. 9C). Such a model built on the basis of the dimerization and oligomerization of T serves to explain the incorporation of 8-N_3GTP into Tβ and Tγ. The resolution of the crystal structure of the disulfide-linked oligomeric conformation of T would likely be of great significance for interested crystallographers.

We also showed that Cys-135 was modified with [^{3}H] IAA in the disulfide-linked Tα sample, both in the absence and in the presence of 2 mM DTT. The accessibility of Cys-135 of Tα under both conditions revealed that this residue is not involved in the spontaneous formation of disulfide bonds in Tα. The environment around residue 135 clearly has been slightly altered in Tα, when compared to T, since this residue is not alkylated in the holoenzyme [8]. However, Cys-347 and Cys-135 were modified when Tα-GDP or Tα-GTPγS was incubated with IAA [8]. Cys135 of Tα is located in the short helix αD, which conforms part of TαAH, and is not in direct contact with the Tβγ-complex in the crystal structure of T [34]. Therefore, an indirect steric hindrance originated by the Tβγ-dimer must block the modification of this residue in the holoenzyme. When Tα has been dissociated from Tβγ, the modification of Cys135 is probably permitted by subtle conformational changes in its immediate environment that generate a more accessible residue. As shown previously [8] and again here, these changes can be detected and mapped by chemical alkylation with IAA.

The formation of intermolecular disulfide linkages in Tα could result from a native oligomeric assembly of T or alternatively by an artificial cross-linking between random collision complexes of T heterotrimers. However, it has been reported that at concentrations of protein below 10 μM, no significant accidental intermolecular cross-linking between separate molecules of protein occurs when a solution of protein is mixed with a cross-linking agent [46]. Instead, the product that results from intra-oligomeric cross-linking among the fixed number of polypeptides of which the protein is composed is what is observed. Our experiments with T were carried out at protein concentrations between 0.2 and 6 μM, hindering the probability of accidental or transient collisions between T molecules. Moreover, the cross-linking reported here involved the formation of disulfide bridges, which are covalent bonds formed by a zero-length cross-linking reagent. On the basis of the pKa of the sulfhydryl side chains of cysteinyl residues which is ~8.0, and in view of the fact that the disulfide-linked oligomers of Tα were generated under very mild conditions (pH 6.8), it clearly seems that the Cys pairs participating in the formation of these disulfide bridges require to be located in close proximity or at adjacent positions in the protein. These facts strongly imply that the cross-linked disulfide products probably reflect a stable association between native T heterotrimes rather than a random interaction, and suggest a dimeric/oligomeric structure for T similar to the model proposed in Fig. 9C.

Results from analytical ultracentrifugation and native gel electrophoresis have also suggested the presence of oligomeric states of

T and its subunits [47]. Consistent with these findings are kinetic studies of the Rho-catalyzed guanine nucleotide exchange [48], as well as binding studies between the photoreceptor protein and T [49], which demonstrate allosteric regulation of the interaction of T with photolyzed Rho. The molecular basis for the positive cooperative behavior was hypothesized to involve oligomeric associations of T. Another means of assessing the structure of T is to examine the nearest-neighbor relationships of the components with the use of cross-linking agents. If multimeric structures of T exist, they should be susceptible to cross-linking, yielding structures having much higher molecular weights than T heterotrimers. The chemical cross-linking studies of Hingorani et al. [50] also substantiated the presence of oligomeric forms of transducin. Their results, using bifunctional chemical cross-linkers, indicated that in the GDP-liganded resting state T was in a trimeric $(T\alpha\text{-}T\beta\text{-}T\gamma)_3$ complex, but upon binding of GMP-PNP this complex appeared to be disrupted [50]. T oligomers were also trapped by using *N*,*N*′-1,2-phenylenedlmaleimide and *N*,*N*′-1,4-phenylenedlmaleimide [10], and by 1-ethyl 3-(3-dimethylaminopropyl) carbodiimide-induced cross-linking [11], providing physical evidences for the existence of these oligomers under native conditions. A radioactive and photoactivatable derivative of NAD^+, 2-azido-[adenylate-^{32}P] NAD^+, was employed with pertussis toxin to ADP-ribosylate Cys-347 of Tα [51]. ADP-ribosylation of Tα followed by light activation of the azide moiety of the reagent produced four cross-linked species involving the α and γ subunits of T, namely a Tα trimer $(T\alpha)_3$, a $T\alpha_2$-Tγ cross-link, a Tα dimer $(T\alpha)_2$, and a Tα-Tγ cross-link. Mapping the interacting sites between cross-linked Tα dimers and Tα trimers indicated that the C-terminal domain of Tα is involved in the formation of Tα homopolymers in solution [51]. In contrast to all these studies, a large body of evidence has implicated T heterotrimers as being the structures responsible for Rho-mediated actions in phototransduction. For example, the characterization of purified T by gel filtration [52], sucrose density gradient analysis [52], and neutron scattering [53] have all failed to support the presence of oligomeric forms of the G protein. The discrepancy among these various approaches suggests that the oligomeric associations may be fairly labile and sensitive to the conditions imposed by the various techniques.

Evidences for the oligomerization of other heterotrimeric G proteins different than T have also been described. Target size analysis was employed as a means of determining the functional size of the transduction systems in various native membranes. In the case of the glucagon-sensitive adenylyl cyclase system in rat liver membranes, it was ascertained by Schlegel et al. [54] that the functional size of the system prior to activation was 4-fold higher than when the system was activated. It was then postulated by Rodbell [55] that the activation process might involve the breakdown of a putative multimeric structure involving the stimulatory G protein Gs to smaller structures. The adenylyl cyclase system in the plasma membrane of fat cells also contains G protein components that either stimulate or inhibit activity in response to ligands acting at the cell surface. Schlegel et al. [56] have analyzed the effects of high-energy radiation on the stimulatory and inhibitory processes and conclude that these processes were mediated by structures of different functional size. Since similar target sizes were found for the system inhibited by the α-subunit of the inhibitory G protein Gi in rat adipocytes [56], it seemed possible that this mechanism might apply generally to transduction systems involving G proteins. Nakamura and Rodbell [57] have reported that various α subunits of G proteins extracted with the detergent *n*-octyl-β-D-glucopyranoside (octyl glucoside) from rat brain synaptoneurosomes behaved hydrodynamically on sucrose gradients as large polydisperse structures having sedimentation values far larger than those exhibited by heterotrimeric G proteins extracted with sodium cholate or lubrol, the usual detergents employed for extraction and purification [58]. Nakamura and Rodbell [59] also reported that similar large structures of $G\alpha_s$ were extracted with octyl glucoside from rat hepatocyte membranes containing glucagon receptors. Glucagon, in the presence of GTPγS, rapidly and selectively induced conversion of the large structures of $G\alpha_s$ into smaller structures. It became apparent that G proteins do not exist only as heterotrimers; depending on the type of detergent used in their extraction, they can also exist as multimers of varying size and sensitivity to the activating effects of guanine nucleotides. Moreover, Coulter and Rodbell [60] have treated rat brain synaptoneurosomes with *N*,*N*′-1,4-phenylenedlmaleimide under conditions that caused extensive cross-linking of the α and β subunits of three major types of heterotrimeric G proteins (Go, Gs, Gi) present in brain membranes. The major cross-linked products were coeluted from Bio-Gel sizing columns as very large structures that did not penetrate stacking gels during separations by SDS-PAGE. The α subunits but not the βγ-complexes of Gs, Go, and Gi also yielded cross-linked products of intermediate sizes. None of the products were as small as the heterotrimeric G proteins extracted from brain by cholate or lubrol. Yet, the large and intermediate cross-linked structures were strikingly similar to the large, polydisperse structures of the α subunits of Gs, Gi and Go extracted from synaptoneurosomes by octyl glucoside, which have sedimentation properties of multimeric proteins.

Through proximity, the speed and selectivity of binding interactions between proteins can be vastly improved, leading to higher cellular efficiency. Examples include the proteasome for molecular degradation, the metabolon for oxidative energy generation, and the ribosome for protein synthesis. Only a small fraction of proteins function in isolation, while the majority of proteins form complexes with identical or very similar chains (homooligomers) or with different non-homologous chains (heterooligomers) [61–63]. Unfortunately, many of the techniques used to break open cells and isolate proteins are inherently disruptive to large multiprotein complexes, so these complexes within the cell may be even more widespread than can be detected. Protein oligomerization and transitions between different oligomeric states may provide the diversity and specificity of many pathways and may mediate and regulate gene expression, activity of enzymes, ion channels, receptors, and cell–cell adhesion processes [64–70]. It has also been suggested that large assemblies consisting of many identical subunits have advantageous regulatory properties as they can undergo sensitive phase transitions [71]. Formation of oligomers can also provide sites for allosteric regulation, generate new binding sites at interfaces to enhance specificity, and increase diversity in the generation of regulatory complexes [72]. In addition, oligomerization allows proteins to form large structures without increasing genome size and provides stability, while the reduced surface area of the monomer in a complex can offer protection against denaturation [71,73,74]. On the basis of all these advantages that have been recognized in other systems, multimeric arrangements of T probably will physiologically benefit the phototransduction process. In the classical collision-coupling mechanistic view of phototransduction, the different components of its biochemical machinery have been modeled as freely diffusing monomeric molecules in the lipid milieu of the rod discs. Results published in recent years threaten to significantly complicate this picture. High resolution atomic force microscopy and electron microscopy performed on native mouse rod discs led to the surprising result that Rho is organized in highly dense arrays of dimers that overall form paracrystalline rafts of receptors [75–77]. These results were corroborated by several biochemical techniques [78–81] and by high speed dichroic microspectrophotometric measurements [82]. In particular, microspectrophotometry analysis proved

that significant amounts of immobile Rho were present in native discs, hence suggesting large areas of paracrystalline assemblies of Rho [82]. Dell'Orco and Koch [83] investigated the kinetics of interaction between native Rho and T by surface plasmon resonance and analyzed the results in the general physiological context by employing a holistic systems modeling approach. Their results point to a mechanism that is intermediate between pure collisional coupling and physical scaffolding. Such dynamic scaffolding, in which prevalently dimeric Rho and T interact in the dark by forming transient complexes, does not slow down the phototransduction cascade, but is compatible with the observed photoresponses on a broad scale of light stimuli [83,84]. On the basis of the putative oligomeric organization of Rho, it will be interesting to evaluate whether the formation of multimers of T also play a key role in the dynamics of Rho-T interaction and in the complex supramolecular organization seen in rod outer segment disks.

5. Conclusions

A connection has been found between the ptotoaffinity labeling of transducin with 8-N_3GTP and the spontaneous formation of interchain disulfide bonds involving its α subunit. A model was built based on the dimerization and oligomerization of transducin heterotrimers via disulfide cross-linking of their α subunit protomers, which enlightens the covalent incorporation of 8-N_3GTP into all three subunits of the protein.

Conflict of interests

The authors declare that there is no conflict of interests regarding the publication of this article.

Authors' contributions

J.B. designed research. D.P., C.M., and J.B. performed research, analyzed data and wrote the paper. All authors read and approved the final manuscript.

Acknowledgments

This work was supported by grants N° S1-2000000514 and N° LAB-2000001639 from FONACIT, Caracas, Venezuela; and N° S1-IN-CB-001-09 from Decanato de Investigación y Desarrollo, Universidad Simón Bolívar, Caracas, Venezuela. We want to thank Barry Knox, State University of New York, Syracuse, USA, for supplying the 1D4-Sepharose and 1′-18′ competing synthetic peptide used for the purification of Rho, and Ricardo Guzmán for helping with the illustrations.

References

[1] P.A. Hargrave, Rhodopsin structure, function, and topography the Friedenwald lecture, Invest. Ophthalmol. Vis. Sci. 42 (2001) 3–9.
[2] J.F. Wilkins, M.W. Bitensky, B.M. Willardson, Regulation of the kinetics of phosducin phosphorylation in retinal rods, J. Biol. Chem. 271 (1996) 19232–19237.
[3] F. Chen, R.H. Lee, Phosducin and βγ-transducin interaction I: effects of post-translational modifications, Biochem. Biophys. Res. Commun. 233 (1997) 370–374.
[4] W. He, C.W. Cowan, T.G. Wensel, RGS9, a GTPase accelerator for phototransduction, Neuron 20 (1998) 95–102.
[5] E.R. Makino, J.W. Handy, T. Li, V.Y. Arshavsky, The GTPase activating factor for transducin in rod photoreceptors is the complex between RGS9 and type 5 G protein β subunit, Proc. Natl. Acad. Sci. U. S. A. 96 (1999) 1947–1952.
[6] J. Bubis, H.G. Khorana, Sites of interaction in the complex between β- and γ-subunits of transducin, J. Biol. Chem. 265 (1990) 12995–12999.
[7] J. Bubis, J.O. Ortiz, C. Möller, E.J. Millán, Identification and characterization of transducin functional cysteines, lysines, and acidic residues by group-specific labeling and chemical cross-linking, in: M.Z. Atassi, E. Appella (Eds.), Methods in Protein Structure Analysis, Plenum Press, New York, 1995, pp. 227–250.
[8] J. Bubis, J.O. Ortiz, C. Möller, Chemical modification of transducin with iodoacetic acid: transducin-α carboxymethylated at Cys_{347} allows transducin binding to rhodopsin but prevents its release in the presence of GTP, Arch. Biochem. Biophys. 395 (2001) 146–157.
[9] J.O. Ortiz, J. Bubis, Effects of differential sulfhydryl group-specific labeling on the rhodopsin and guanine nucleotide binding activities of transducin, Arch. Biochem. Biophys. 387 (2001) 233–242.
[10] E.J. Millán, J. Bubis, Identification of functionally important cysteines in the α-subunit of transducin by chemical cross-linking techniques, J. Protein Chem. 21 (2002) 1–8.
[11] A. Kosoy, C. Möller, D. Perdomo, J. Bubis, Identification of functionally important acidic residues in transducin by group-specific labeling, Biol. Res. 36 (2003) 389–404.
[12] A. Kosoy, C. Möller, D. Perdomo, J. Bubis, Chemical modification of transducin with dansyl chloride hinders its binding to light-activated rhodopsin, J. Biochem. Mol. Biol. 37 (2004) 260–267.
[13] D.J. Takemoto, B.E. Haley, J. Hansen, O. Pinkett, L.J. Takemoto, GTPase from rod outer segments: characterization by photoaffinity labeling and tryptic peptide mapping, Biochem. Biophys. Res. Commun. 102 (1981) 341–347.
[14] M.M. McMurray, J.S. Hansen, B.E. Haley, D.J. Takemoto, L.J. Takemoto, Interspecies conservation of retinal guanosine 5′-triphosphatase. Characterization by photoaffinity labelling and tryptic-peptide mapping, Biochem. J. 225 (1985) 227–232.
[15] R.E. Kohnken, D.G. Mc Connell, Use of 8-azidoguanosine 5′-[γ-^{32}P]triphosphate as a probe of the guanosine 5′-triphosphate binding protein subunits in bovine rod outer segments, Biochemistry 24 (1985) 3803–3809.
[16] V.N. Hingorani, L.F. Ho Chang, Y.K. Ho, Chemical modification of bovine transducin: probing the GTP-binding site with affinity analogues, Biochemistry 28 (1989) 7424–7432.
[17] G. Yamanaka, F. Eckstein, L. Stryer, Stereochemistry of the guanyl nucleotide binding site of transducin probed by phosphorothioate analogues of GTP and GDP, Biochemistry 24 (1985) 8094–8101.
[18] G. Yamanaka, F. Eckstein, L. Stryer, Interaction of retinal transducin with guanosine triphosphate analogues: specificity of the γ-phosphate binding region, Biochemistry 25 (1986) 6149–6153.
[19] D.J. Kelleher, L.W. Dudycz, G.E. Wright, G.L. Johnson, Ability of guanine nucleotide derivatives to bind and activate bovine transducin, Mol. Pharmacol. 30 (1986) 603–608.
[20] M. Jaffé, J. Bubis, Affinity labeling of the guanine nucleotide binding site of transducin by pyridoxal 5′-phosphate, J. Protein Chem. 21 (2002) 339–348.
[21] M. Jaffé, J. Bubis, Use of 5′-[*p*-(fluorosulfonyl)benzoyl] guanosine as an affinity probe for the guanine nucleotide-binding site of transducin, Protein J. 26 (2007) 125–133.
[22] S.E. Frey, V.N. Hingorani, S.M. Su-Tsai, Y.K. Ho, Chromium(III) β,γ-bidentate guanine nucleotide complexes as probes of the GTP-activated cGMP cascade of retinal rod outer segments, Biochemistry 27 (1988) 8209–8218.
[23] J. Bubis, Effect of detergents and lipids on transducin photoactivation by rhodopsin, Biol. Res. 31 (1998) 59–71.
[24] H. Shichi, R.L. Somers, Light-dependent phosphorylation of rhodopsin. Purification and properties of rhodopsin kinase, J. Biol. Chem. 253 (1978) 7040–7046.
[25] G. Wald, P.K. Brown, The molar extinction of rhodopsin, J. Gen. Physiol. 37 (1953) 189–200.
[26] D.D. Oprian, R.S. Molday, R.J. Kaufman, H.G. Khorana, Expression of a synthetic bovine rhodopsin gene in monkey kidney cells, Proc. Natl. Acad. Sci. U. S. A. 84 (1987) 8874–8878.
[27] D. MacKenzie, A. Arendt, P. Hargrave, J.H. McDowell, R.S. Molday, Localization of binding sites for carboxyl terminal specific anti-rhodopsin monoclonal antibodies using synthetic peptides, Biochemistry 23 (1984) 6544–6549.
[28] J. Bubis, Improved purification of transducin subunits from bovine retinal rod outer segments, Biol. Res. 28 (1995) 291–299.
[29] U.K. Laemmli, Cleavage of structural proteins during the assembly of the head of bacteriophage T4, Nature 227 (1970) 680–685.
[30] P. Matsudaira, Sequence from picomole quantities of proteins electroblotted onto polyvinylidene difluoride membranes, J. Biol. Chem. 262 (1987) 10035–10038.
[31] M.M. Bradford, A rapid and sensitive method for the quantitation of microgram quantities of protein utilizing the principle of protein-dye binding, Anal. Biochem. 72 (1976) 248–254.
[32] N. Dhanasekaran, M. Wessling-Resnick, D.J. Kelleher, G.L. Johnson, A.E. Ruoho, Mapping of the carboxyl terminus within the tertiary structure of transducin's α subunit using the heterobifunctional cross-linking reagent, ^{125}I-*N*-(3-iodo-4-azidophenylpropionamido-*S*-(2-thiopyridyl) cysteine, J. Biol. Chem. 263 (1988) 17942–17950.
[33] C.S. Yang, N.P. Skiba, M.R. Mazzoni, H.E. Hamm, Conformational changes at the carboxyl terminus of Gα occur during G protein activation, J. Biol. Chem. 274 (1999) 2379–2385.
[34] D.G. Lambright, J. Sondek, A. Bohm, N.P. Skiba, H.E. Hamm, P.B. Sigler, The 2.0 Å crystal structure of a heterotrimeric G protein, Nature 379 (1996) 311–319.
[35] D.G. Lambright, J.P. Noel, H.E. Hamm, P.B. Sigler, Structural determinants for activation of the α-subunit of a heterotrimeric G protein, Nature 369 (1994) 621–628.

[36] J.P. Noel, H.E. Hamm, P.B. Sigler, The 2.2 Å crystal structure of transducin-α complexed with GTPγS, Nature 366 (1993) 654–663.
[37] S.G. Rasmussen, B.T. DeVree, Y. Zou, A.C. Kruse, K.Y. Chung, T.S. Kobilka, F.S. Thian, P.S. Chae, E. Pardon, D. Calinski, J.M. Mathiesen, S.T. Shah, J.A. Lyons, M. Caffrey, S.H. Gellman, J. Steyaert, G. Skiniotis, W.I. Weis, R.K. Sunahara, B.K. Kobilka, Crystal structure of the β2 adrenergic receptor-Gs protein complex, Nature 477 (2011) 549–555.
[38] R.K. Sunahara, J.J. Tesmer, A.G. Gilman, S.R. Sprang, Crystal structure of the adenylyl cyclase activator Gsα, Science 278 (1997) 1943–1947.
[39] H.E. Hamm, D. Deretic, A. Arendt, P.A. Hargrave, B. Koenig, K.P. Hofmann, Site of G protein binding to rhodopsin mapped with synthetic peptides from the α subunit, Science 241 (1988) 832–835.
[40] E.A. Dratz, J.E. Furstenau, C.G. Lambert, D.L. Thireault, H. Rarick, T. Schepers, S. Pakhlevaniants, H.E. Hamm, NMR structure of a receptor-bound G-protein peptide, Nature 363 (1993) 276–281.
[41] B.R. Conklin, Z. Farfel, K.D. Lustig, D. Julius, H.R. Bourne, Substitution of three amino acids switches receptor specificity of Gqα to that of Giα, Nature 363 (1993) 274–276.
[42] W.F. Simonds, P.K. Goldsmith, J. Codina, C.G. Unson, A.M. Spiegel, Gi2 mediates α_2-adrenergic inhibition of adenylyl cyclase in platelet membranes: *in situ* identification with Gα C-terminal antibodies, Proc. Natl. Acad. Sci. U. S. A. 86 (1989) 7809–7813.
[43] M. Wessling-Resnick, G.L. Johnson, Evidence for oligomeric forms of transducins alpha subunit: formation of intermolecular alpha-alpha disulfide linkages, Biochem. Biophys. Res. Commun. 159 (1989) 651–657.
[44] R.E. West Jr., J. Moss, M. Vaughan, T. Liu, T.Y. Liu, Pertussis toxin-catalyzed ADP-ribosylation of transducin. Cysteine 347 is the ADP-ribose acceptor site, J. Biol. Chem. 260 (1985) 14428–14430.
[45] C. Van Dop, G. Yamanaka, F. Steinberg, R.D. Sekura, C.R. Manclark, L. Stryer, H.R. Bourne, ADP-ribosylation of transducin by pertussis toxin blocks the light-stimulated hydrolysis of GTP and cGMP in retinal photoreceptors, J. Biol. Chem. 259 (1984) 23–26.
[46] G.E. Davies, G.R. Stark, Use of dimethyl suberimidate, a cross-linking reagent, in studying the subunit structure of oligomeric proteins, Proc. Natl. Acad. Sci. U. S. A. 66 (1970) 651–656.
[47] W. Baehr, E.A. Morita, R.J. Swanson, M.L. Applebury, Characterization of bovine rod outer segment G-protein, J. Biol. Chem. 257 (1982) 6452–6460.
[48] M. Wessling-Resnick, G.L. Johnson, Allosteric behavior in transducin activation mediated by rhodopsin. Initial rate analysis of guanine nucleotide exchange, J. Biol. Chem. 262 (1987) 3697–3705.
[49] M. Wessling-Resnick, G.L. Johnson, Transducin interactions with rhodopsin. Evidence for positive cooperative behavior, J. Biol. Chem. 262 (1987) 12444–12447.
[50] V.N. Hingorani, D.T. Tobias, J.T. Henderson, Y.K. Ho, Chemical cross-linking of bovine retinal transducin and cGMP phosphodiesterase, J. Biol. Chem. 263 (1988) 6916–6926.
[51] R.R. Vaillancourt, N. Dhanasekaran, G.L. Johnson, A.E. Ruoho, 2-Azido-[^{32}P] NAD^+, a photoactivatable probe for G-protein structure: evidence for holotransducin oligomers in which the ADP-ribosylated carboxyl terminus of α interacts with both α and γ subunits, Proc. Natl. Acad. Sci. U. S. A. 87 (1990) 3645–3649.
[52] M. Wessling-Resnick, G.L. Johnson, Kinetic and hydrodynamic properties of transducin: comparison of physical and structural parameters for GTP-binding regulatory proteins, Biochemistry 26 (1987) 4316–4323.
[53] P. Deterre, J. Bigay, C. Pfister, M. Chabre, Guanine nucleotides and magnesium dependence of the association states of the subunits of transducin, FEBS Lett. 178 (1984) 228–232.
[54] W. Schlegel, E.S. Kempner, M. Rodbell, Activation of adenylate cyclase in hepatic membranes involves interactions of the catalytic unit with multimeric complexes of regulatory proteins, J. Biol. Chem. 254 (1979) 5168–5176.
[55] M. Rodbell, The role of hormone receptors and GTP-regulatory proteins in membrane transduction, Nature 284 (1980) 17–22.
[56] W. Schlegel, D.M. Cooper, M. Rodbell, Inhibition and activation of fat cell adenylate cyclase by GTP is mediated by structures of different size, Arch. Biochem. Biophys. 201 (1980) 678–682.
[57] S. Nakamura, M. Rodbell, Octyl glucoside extracts GTP-binding regulatory proteins from rat brain " synaptoneurosomes" as large, polydisperse structures devoid of βγ complexes and sensitive to disaggregation by guanine nucleotides, Proc. Natl. Acad. Sci. U. S. A. 87 (1990) 6413–6417.
[58] J. Codina, D.J. Carty, L. Birnbaumer, R. Iyengar, Purification of G proteins, Meth. Enzymol. 195 (1991) 177–188.
[59] S. Nakamura, M. Rodbell, Glucagon induces disaggregation of polymer-like structures of the α subunit of the stimulatory G protein in liver membranes, Proc. Natl. Acad. Sci. U. S. A. 88 (1991) 7150–7154.
[60] S. Coulter, M. Rodbell, Heterotrimeric G proteins in synaptoneurosome membranes are crosslinked by p-phenylenedimaleimide, yielding structures comparable in size to crosslinked tubulin and F-actin, Proc. Natl. Acad. Sci. U. S. A. 89 (1992) 5842–5846.
[61] J.B. Pereira-Leal, E.D. Levy, S.A. Teichmann, The origins and evolution of functional modules: lessons from protein complexes, Philos. Trans. R. Soc. Lond. B Biol. Sci. 361 (2006) 507–517.
[62] K. Hashimoto, H. Nishi, S. Bryant, A.R. Panchenko, Caught in self-interaction: evolutionary and functional mechanisms of protein homooligomerization, Phys. Biol. 8 (2011) 035007, http://dx.doi.org/10.1088/1478-3975/8/3/035007.
[63] H. Nishi, K. Hashimoto, T. Madej, A.R. Panchenko, Evolutionary, physicochemical, and functional mechanisms of protein homooligomerization, Prog. Mol. Biol. Transl. Sci. 117 (2013) 3–24.
[64] J.M. Woodcock, J. Murphy, F.C. Stomski, M.C. Berndt, A.F. Lopez, The dimeric versus monomeric status of 14-3-3ζ is controlled by phosphorylation of Ser^{58} at the dimer interface, J. Biol. Chem. 278 (2003) 36323–36327.
[65] S. Mazurek, C.B. Boschek, F. Hugo, E. Eigenbrodt, Pyruvate kinase type M2 and its role in tumor growth and spreading, Semin. Cancer Biol. 15 (2005) 300–308.
[66] R. Koike, A. Kidera, M. Ota, Alteration of oligomeric state and domain architecture is essential for functional transformation between transferase and hydrolase with the same scaffold, Protein Sci. 18 (2009) 2060–2066.
[67] L. Baisamy, N. Jurisch, D. Diviani, Leucine zipper-mediated homo-oligomerization regulates the Rho-GEF activity of AKAP-Lbc, J. Biol. Chem. 280 (2005) 15405–15412.
[68] C.P. Chen, S. Posy, A. Ben-Shaul, L. Shapiro, B.H. Honig, Specificity of cell-cell adhesion by classical cadherins: critical role for low-affinity dimerization through β-strand swapping, Proc. Natl. Acad. Sci. U. S. A. 102 (2005) 8531–8536.
[69] T. Hattori, N. Ohoka, Y. Inoue, H. Hayashi, K. Onozaki, C/EBP family transcription factors are degraded by the proteasome but stabilized by forming dimer, Oncogene 22 (2003) 1273–1280.
[70] P. Katsamba, K. Carroll, G. Ahlsen, F. Bahna, J. Vendome, S. Posy, M. Rajebhosale, S. Price, T.M. Jessell, A. Ben-Shaul, L. Shapiro, B.H. Honig, Linking molecular affinity and cellular specificity in cadherin-mediated adhesion, Proc. Natl. Acad. Sci. U. S. A. 106 (2009) 11594–11599.
[71] D.S. Goodsell, A.J. Olson, Structural symmetry and protein function, Annu. Rev. Biophys. Biomol. Struct. 29 (2000) 105–153.
[72] J.P. Changeux, S.J. Edelstein, Allosteric mechanisms of signal transduction, Science 308 (2005) 1424–1428.
[73] S. Jones, J.M. Thornton, Protein-protein interactions: a review of protein dimer structures, Prog. Biophys. Mol. Biol. 63 (1995) 31–65.
[74] S. Miller, A.M. Lesk, J. Janin, C. Chothia, The accessible surface area and stability of oligomeric proteins, Nature 328 (1987) 834–836.
[75] D. Fotiadis, Y. Liang, S. Filipek, D.A. Saperstein, A. Engel, K. Palczewski, Atomic-force microscopy: rhodopsin dimers in native disc membranes, Nature 421 (2003) 127–128.
[76] D. Fotiadis, Y. Liang, S. Filipek, D.A. Saperstein, A. Engel, K. Palczewski, The G protein-coupled receptor rhodopsin in the native membrane, FEBS Lett. 564 (2004) 281–288.
[77] Y. Liang, D. Fotiadis, S. Filipek, D.A. Saperstein, K. Palczewski, A. Engel, Organization of the G protein-coupled receptors rhodopsin and opsin in native membranes, J. Biol. Chem. 278 (2003) 21655–21662.
[78] R. Medina, D. Perdomo, J. Bubis, The hydrodynamic properties of dark and light-activated states of n-dodecyl-β-D-maltoside-solubilized bovine rhodopsin support the dimeric structure of both conformations, J. Biol. Chem. 279 (2004) 39565–39573.
[79] K. Suda, S. Filipek, K. Palczewski, A. Engel, D. Fotiadis, The supramolecular structure of the GPCR rhodopsin in solution and native disc membranes, Mol. Membr. Biol. 21 (2004) 435–446.
[80] S.E. Mansoor, K. Palczewski, D.L. Farrens, Rhodopsin self-associates in asolectin liposomes, Proc. Natl. Acad. Sci. U. S. A. 103 (2006) 3060–3065.
[81] S.A. Shukolyukov, Aggregation of frog rhodopsin to oligomers and their dissociation to monomer: application of BN- and SDS-PAGE, Biochemistry (Mosc.) 74 (2009) 599–604.
[82] V.I. Govardovskii, D.A. Korenyak, S.A. Shukolyukov, L.V. Zueva, Lateral diffusion of rhodopsin in photoreceptor membrane: a reappraisal, Mol. Vis. 15 (2009) 1717–1729.
[83] D. Dell'Orco, K.W. Koch, A dynamic scaffolding mechanism for rhodopsin and transducin interaction in vertebrate vision, Biochem. J. 440 (2011) 263–271.
[84] D. Dell'Orco, A physiological role for the supramolecular organization of rhodopsin and transducin in rod photoreceptors, FEBS Lett. 587 (2013) 2060–2066.